Supporting Information

Mechanism of the AppA$_{BLUF}$ Photocycle Probed by Site-Specific Incorporation of Fluorotyrosine Residues: The Effect of the Y21 pKa on the Forward and Reverse Ground-State Reactions

Agnieszka A. Gil[‡], Allison Haigney[‡], Sergey P. Laptenok[§], Richard Brust[‡], Andras Lukacs[¶], James N. Iuliano[‡], Jessica Jeng[‡], Eduard H. Melief[‡], Rui-Kun Zhao[§], Eunbin Yoon[‡], Ian P. Clark[‖], Michael Towrie[‖], Gregory M. Greetham[‖], Annabelle Ng[†], James J. Truglio[†], Jarrod B. French[‡,¥], Stephen R. Meech[§,*] and Peter J. Tonge[‡,*]

[‡]Department of Chemistry, and [¥]Biochemistry & Cell Biology, Stony Brook University, Stony Brook, New York 11794-3400, USA; [†]William A. Shine Great Neck South High School, 341 Lakeville Rd, Great Neck, NY 11020, USA; [¶]Department of Biophysics, Medical School, Szigeti Strasse 12, H-7624 Pécs, Hungary; [§]School of Chemistry, University of East Anglia, Norwich Research Park, Norwich NR4 7TJ, UK; [‖]Central Laser Facility, Harwell Science and Innovation Campus, Didcot, Oxon OX11 0QX, UK.

Supplementary Tables and Figures

Table S1. pH dependence of the light to dark state recovery in wild-type and FY21 AppA$_{BLUF(Y56F)}$.

	Recovery Rate /s^{-1}				
	pH6/pD6	**pH7/pD7**	**pH8/pD8**	**pH9/pD9**	**pH10/pD10**
AppA$_{BLUF}$	ND	7.3 x 10^{-4}/ND	6.5 x 10^{-4}/1.3 x 10^{-4}	7.5 x 10^{-4}/ND	ND
AppA$_{BLUF(Y56F)}$	ND	6.0 x 10^{-4}/ND	6.5 x 10^{-4}/1.3 x 10^{-4}	6.4 x 10^{-4}/ND	ND
2-FY21 AppA$_{BLUF(Y56F)}$	ND	1.3 x 10^{-2}/ND	1.1 x 10^{-2}/1.8 x 10^{-3}	1.2 x 10^{-2}/ND	ND
3-FY21 AppA$_{BLUF(Y56F)}$	ND	3.6 x 10^{-2}/4.9 x 10^{-3}	3.4 x 10^{-2}/3.9 x 10^{-3}	3.7 x 10^{-2}/ND	ND
2,3-F_2Y21 AppA$_{BLUF(Y56F)}$	0.26/ND	0.22/0.39	0.22/0.04	0.24/0.045	0.3/0.06
3,5-F_2Y21 AppA$_{BLUF(Y56F)}$	0.5/0.15	0.56/0.13	0.63/0.11	0.69/0.13	0.75/0.15
2,3,5-F_3Y21 AppA$_{BLUF(Y56F)}$	2.7/1.48	2.9/1.21	2.6/1.15	2.7/1.16	ND/1.18

[1]ND: The recovery rate was not determined at pH6/pD6 or pH10/pD10 for all samples. In some cases this was due to the impact of pH on protein stability.

Figure S1. Mass spectra of 2-FY, 3-FY, 2,3-F_2Y, 3,5-F_2Y, and 2,3,5-F_3Y.

A) 2-FY. Mass (M+H) calculated for $C_9H_{11}FNO_3$ 200.07, found 200.1.

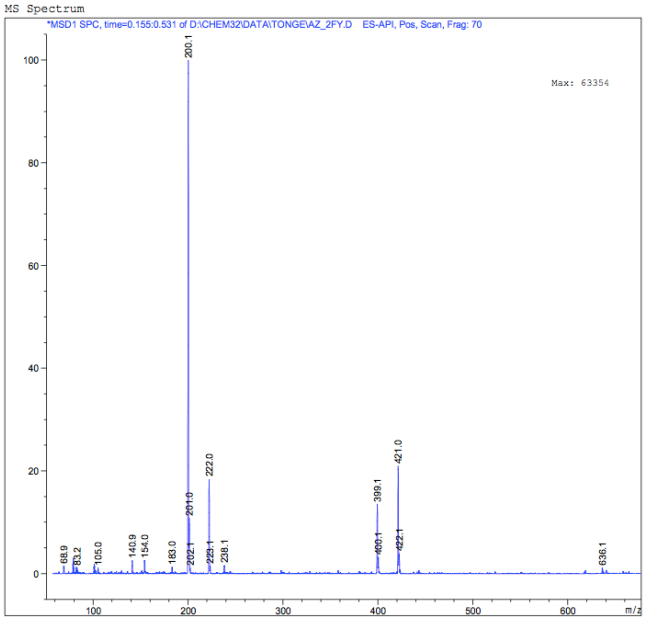

B) 3-FY Mass (M+H) calculated for $C_9H_{11}FNO_3$ 200.07, found 200.0.

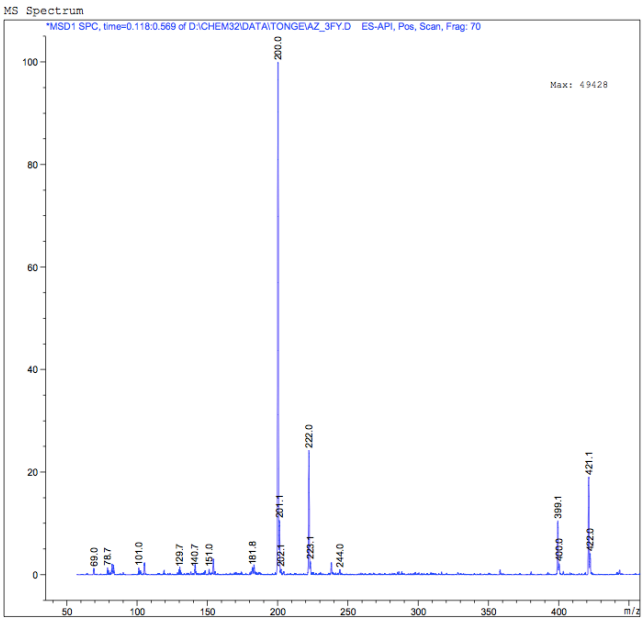

C) 2,3-F_2Y Mass (M+H) calculated for $C_9H_{10}F_2NO_3$ 218.1, found 218.0.

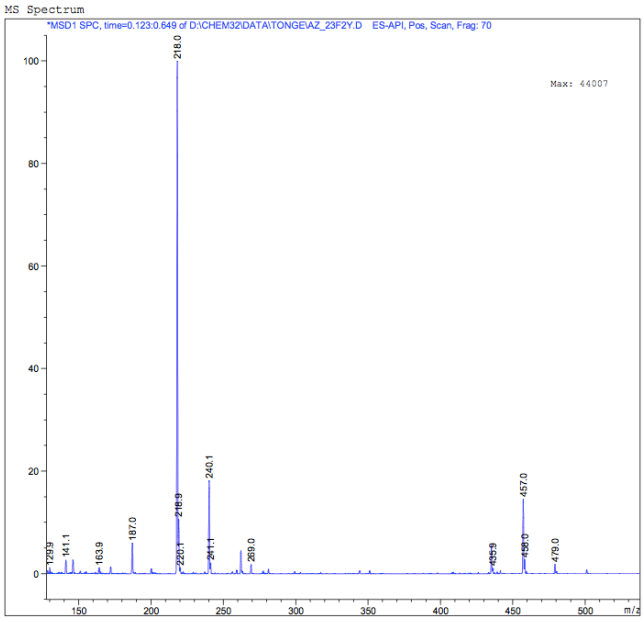

D) 3,5-F_2Y Mass (M+H) calculated for $C_9H_{10}F_2NO_3$ 218.1, found 218.1.

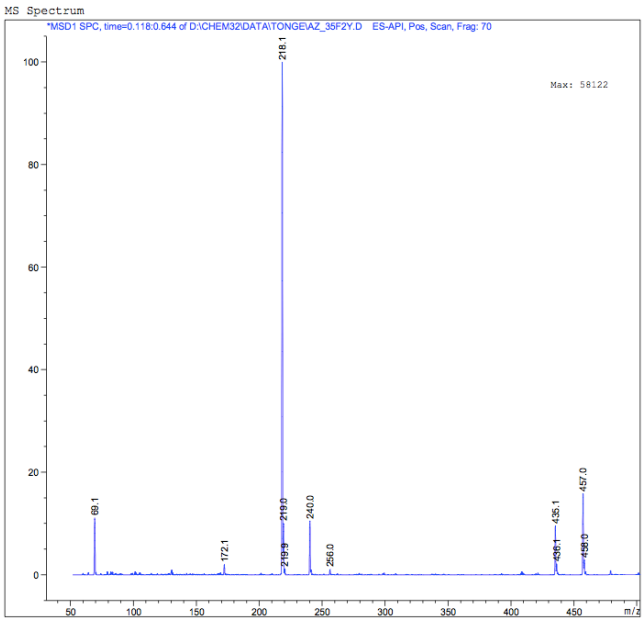

E) 2,3,5-F_3Y Mass (M+H) calculated for $C_9H_9F_3NO_3$ 236.05, found 236.0.

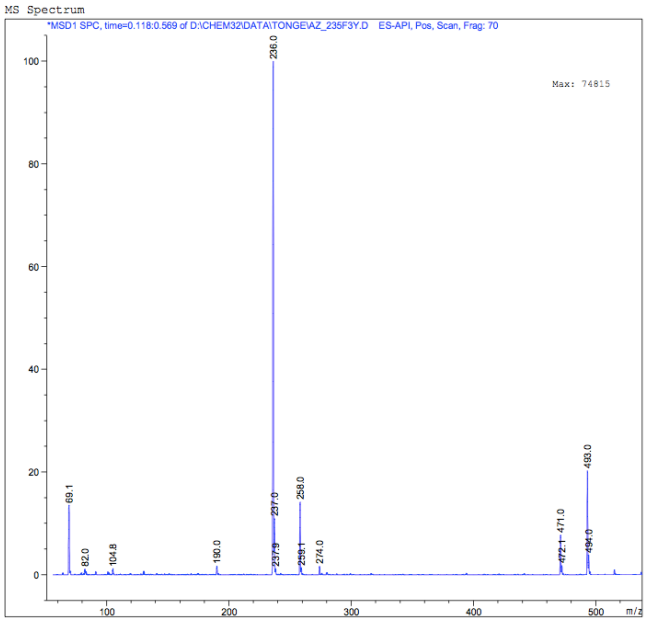

Figure S2. ^{1}H NMR and ^{19}F NMR of the Fluorotyrosines in D_2O.

A) 2-FY

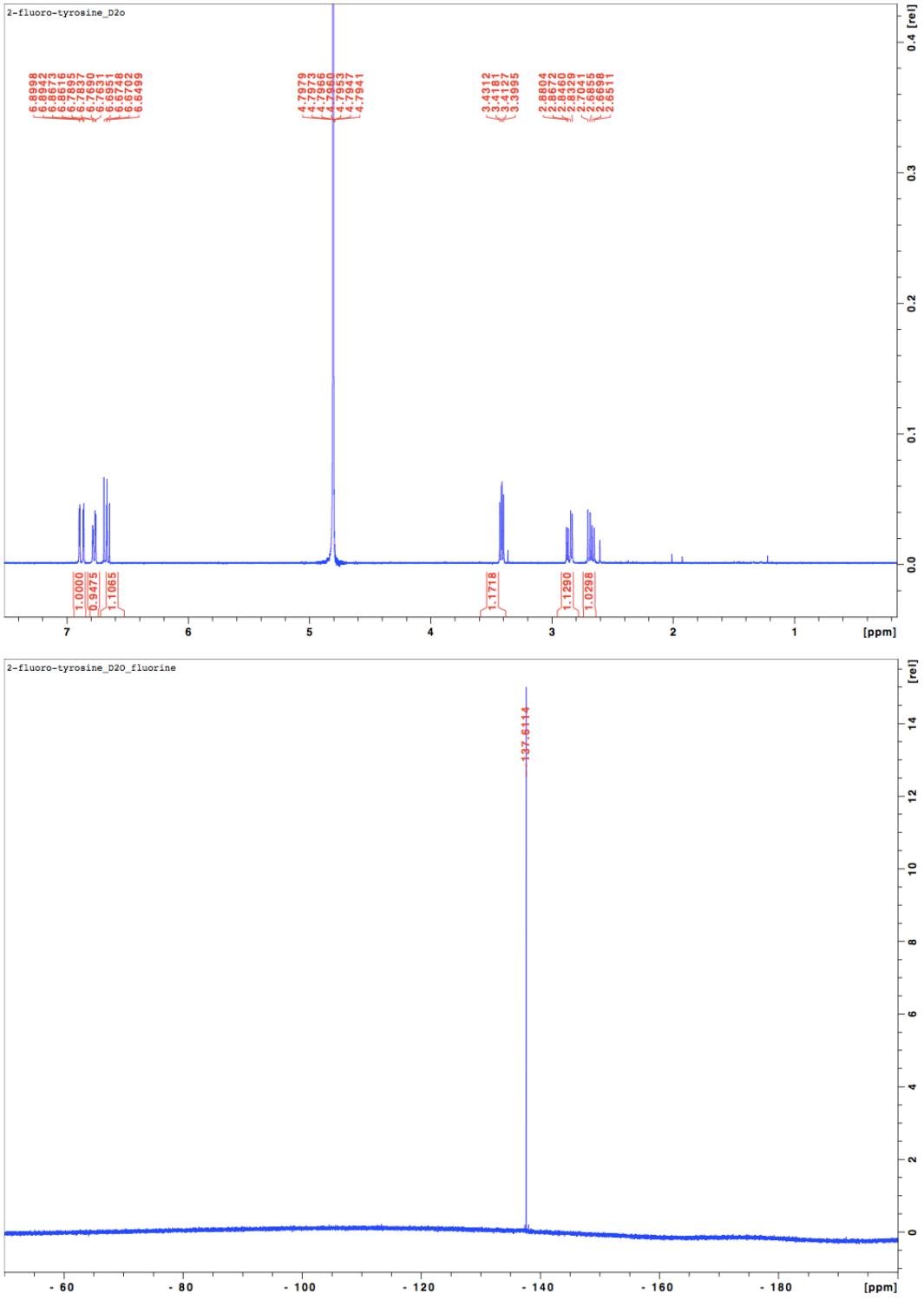

B) 3-FY

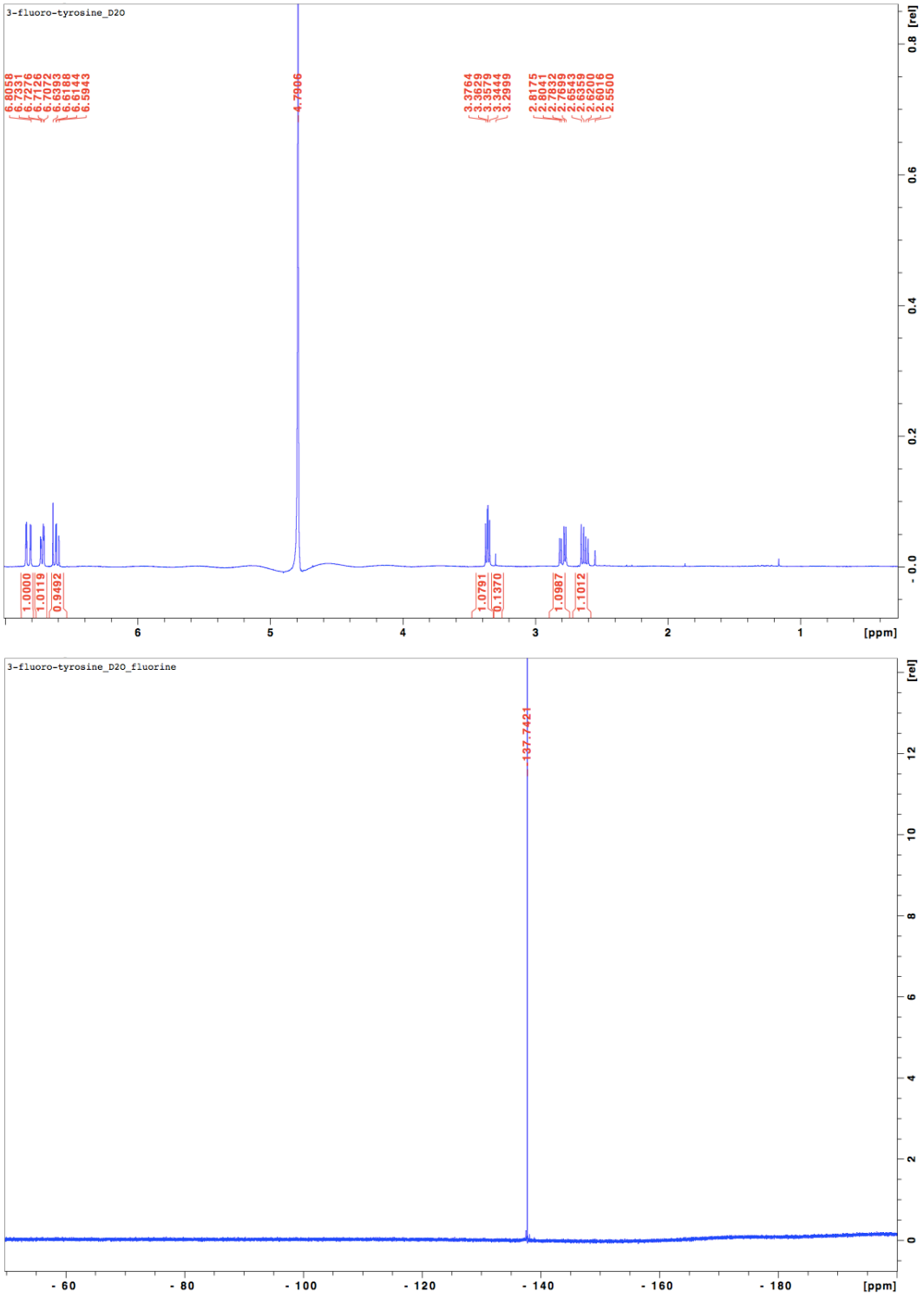
3-fluoro-tyrosine_D2O
6.8058
6.7231
6.7276
6.7126
6.7072
6.6393
6.6288
6.6144
6.5943
4.7906
3.3764
3.3629
3.3579
3.3444
3.2999
2.8175
2.8041
2.7832
2.7699
2.6543
2.6359
2.6210
2.6116
2.5500
1.0000
1.0119
0.9492
1.0791
0.1370
1.0987
1.1012
[ppm]
[rel]
3-fluoro-tyrosine_D2O_fluorine
137.7421
- 60
- 80
- 100
- 120
- 140
- 160
- 180
[ppm]
[rel]

C) 2,3-F_2Y

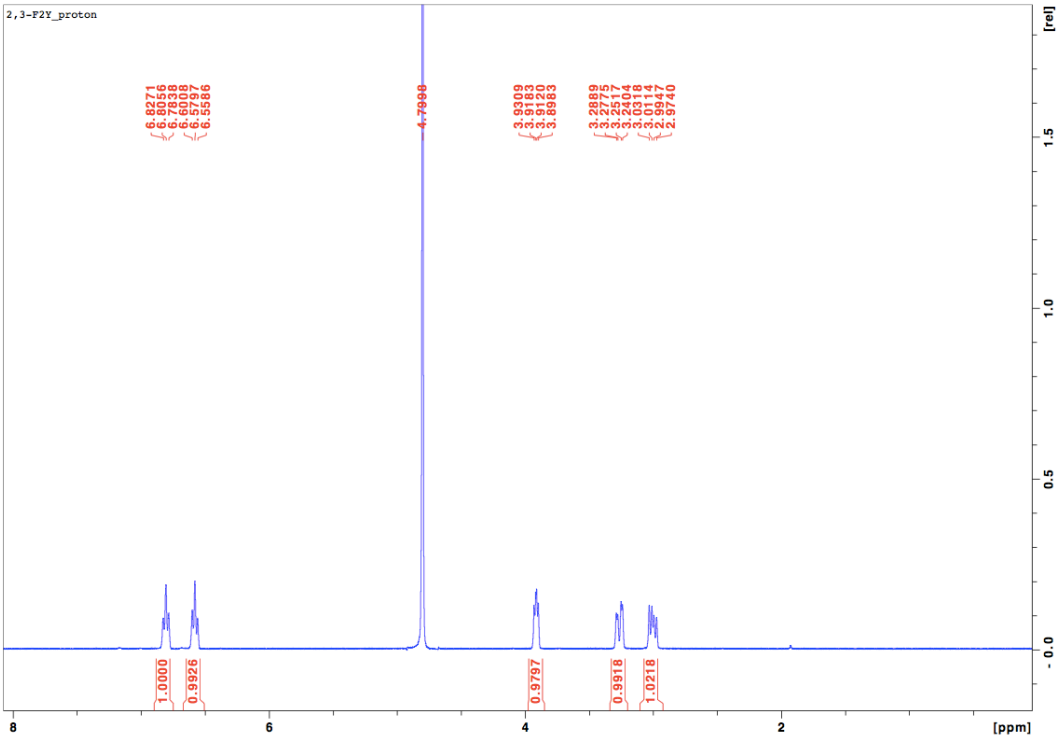
2,3-F2Y_proton
6.8271
6.8056
6.7838
6.6008
6.5797
6.5586
4.7998
3.9309
3.9183
3.9120
3.8983
3.2889
3.2775
3.2517
3.2404
3.0318
3.0114
2.9947
2.9740
1.0000
0.9926
0.9797
0.9918
1.0218
[rel]
[ppm]

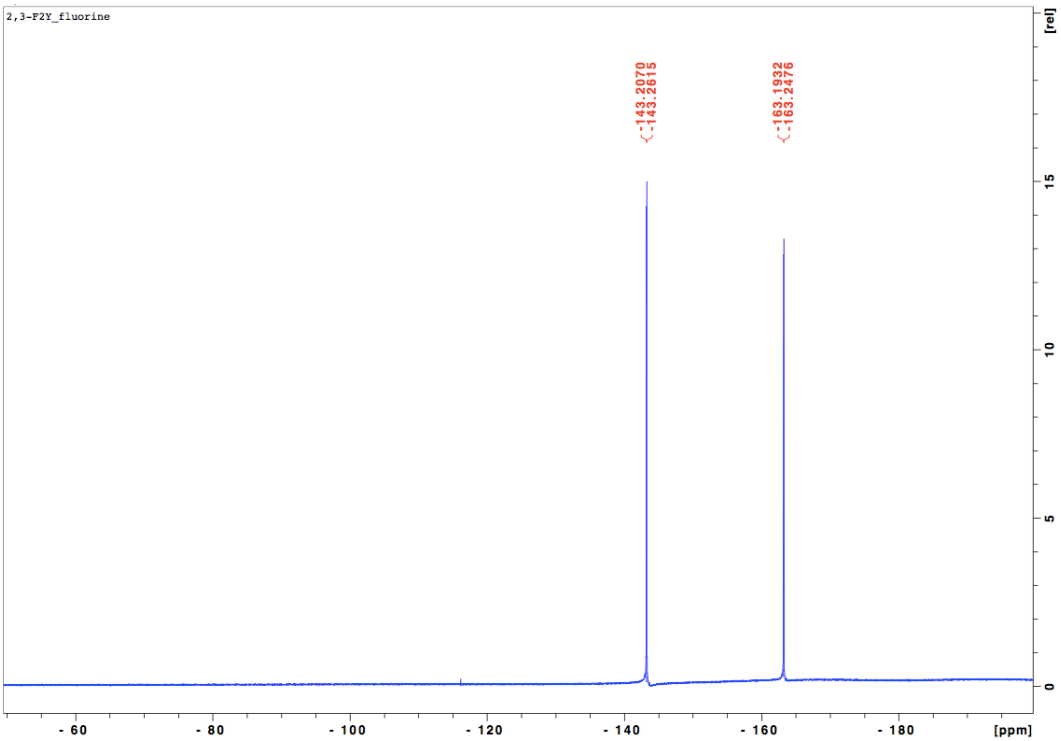
2,3-F2Y_fluorine
-143.2070
-143.2615
-163.1932
-163.2476
[rel]
[ppm]

D) 3,5-F_2Y

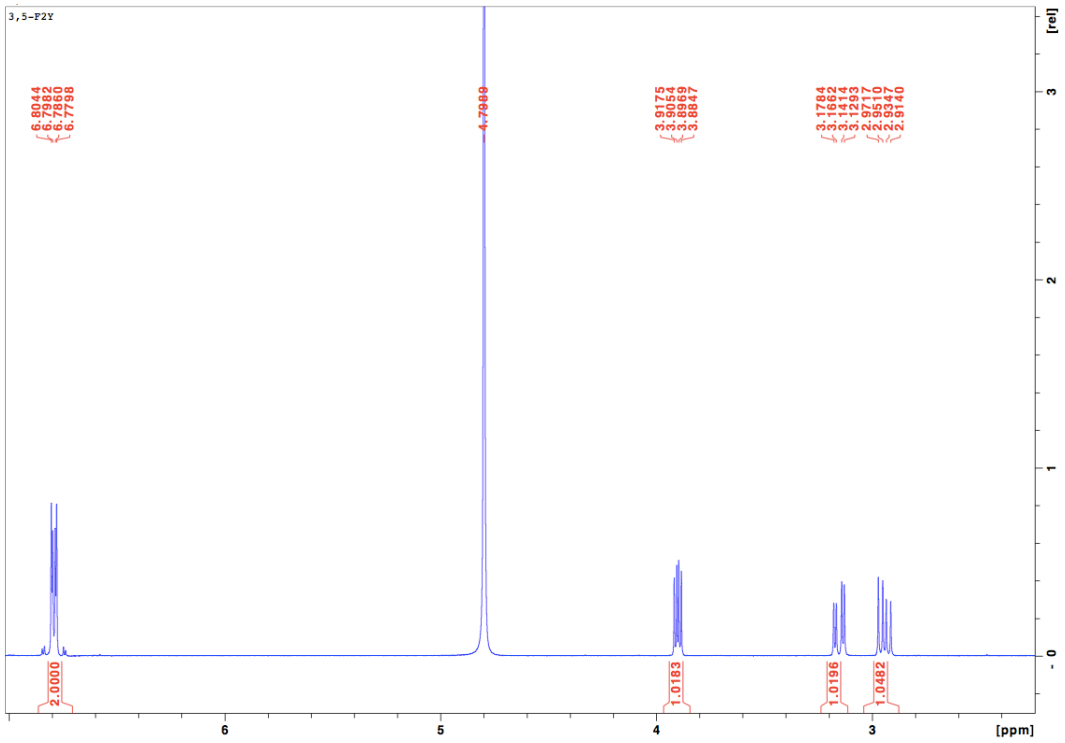
3,5-F2Y
6.8044
6.7982
6.7860
6.7798
4.7000
3.9175
3.9054
3.8969
3.8847
3.1784
3.1662
3.1414
3.1293
2.9717
2.9510
2.9347
2.9140
2.0000
1.0183
1.0196
1.0482
[rel]
[ppm]

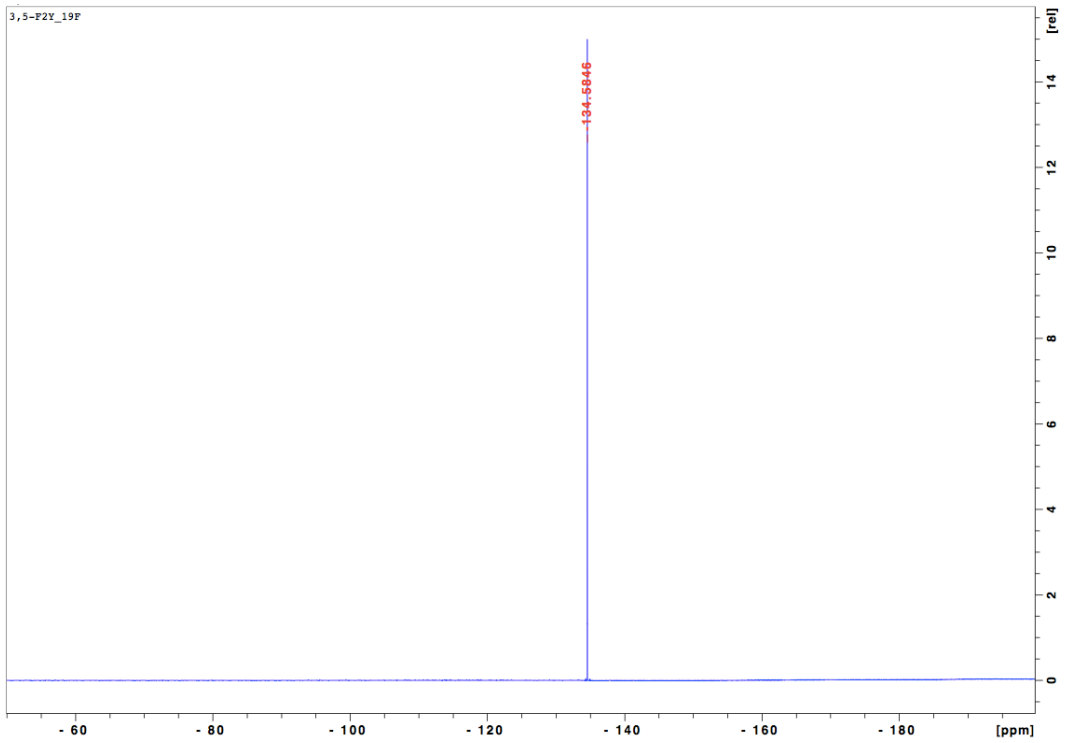
3,5-F2Y_19F
-134.5846
[rel]
[ppm]

E) 2,3,5-F$_3$Y

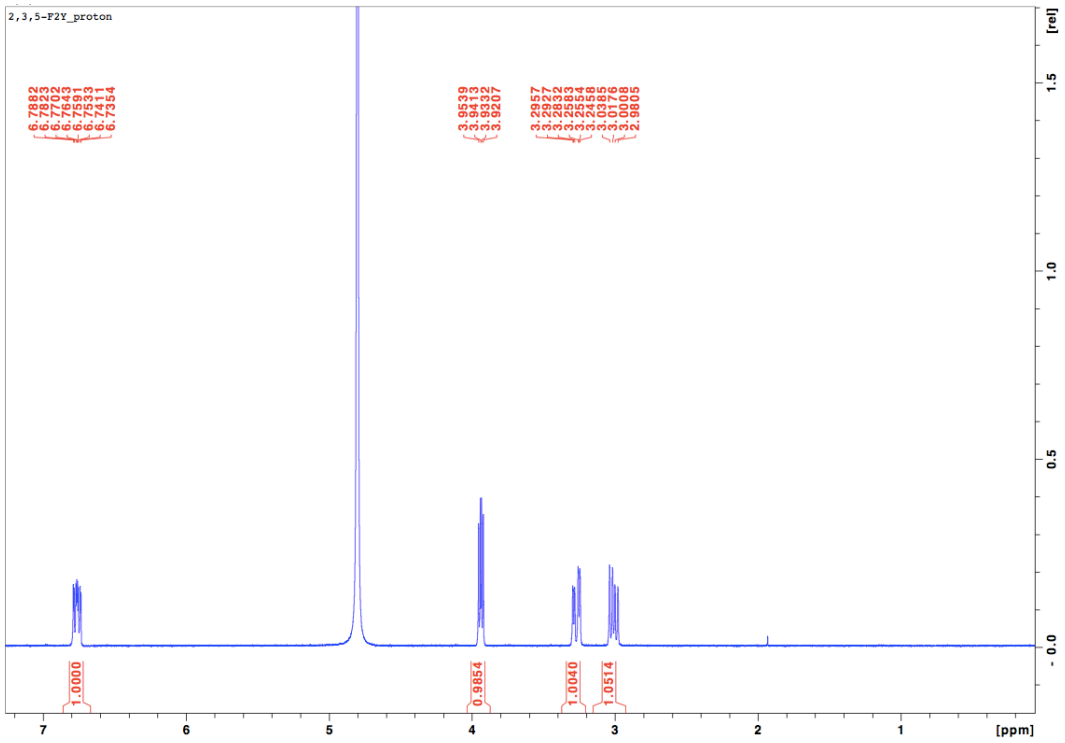
2,3,5-F2Y_proton
6.7882
6.7823
6.7702
6.7643
6.7591
6.7533
6.7411
6.7354
3.9539
3.9413
3.9332
3.9207
3.2957
3.2927
3.2832
3.2583
3.2554
3.2458
3.0385
3.0176
3.0008
2.9805
1.0000
0.9854
1.0040
1.0514
[rel]
[ppm]

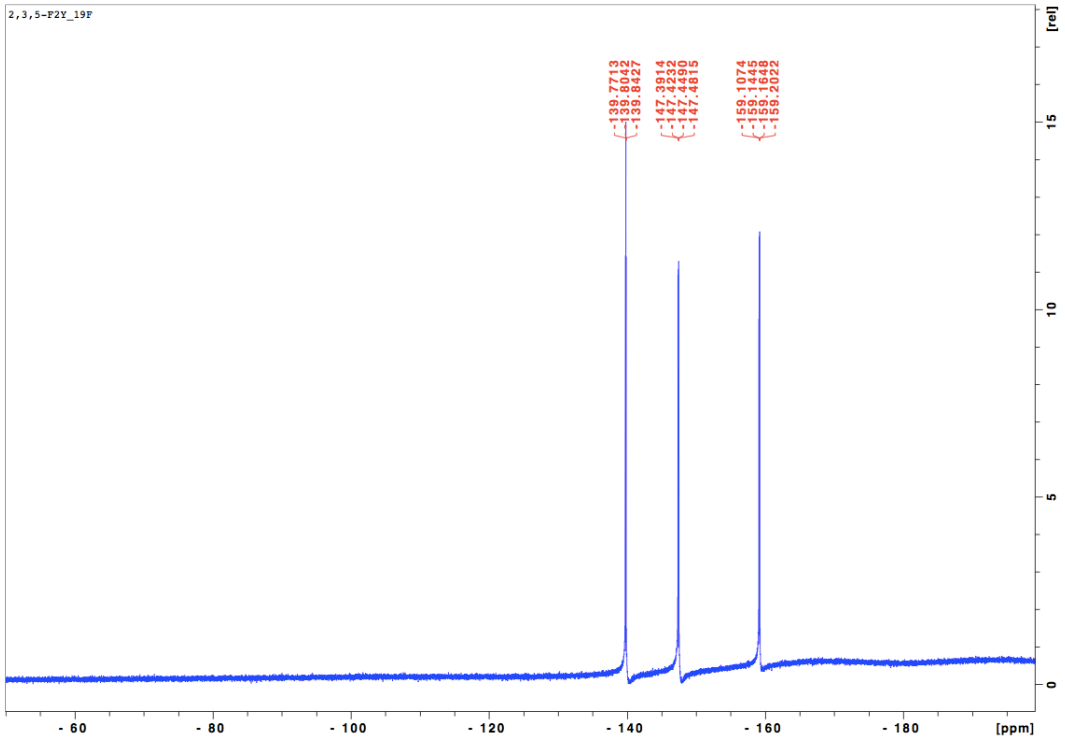
2,3,5-F2Y_19F
-139.7713
-139.8042
-139.8427
-147.3914
-147.4232
-147.4490
-147.4815
-159.1074
-159.1445
-159.1748
-159.2022
[rel]
[ppm]

Figure S3. UV-Vis spectrum of AppA$_{BLUF(Y56F)}$ in the dark state showing the protein/flavin peak at 270 nm and flavin peak at 446 nm.

Chromophore content was determined by taking the ratio of the absorbance at 270 nm and 446 nm. In the representative spectrum below the ratio is 4.2 (1.94/0.46).

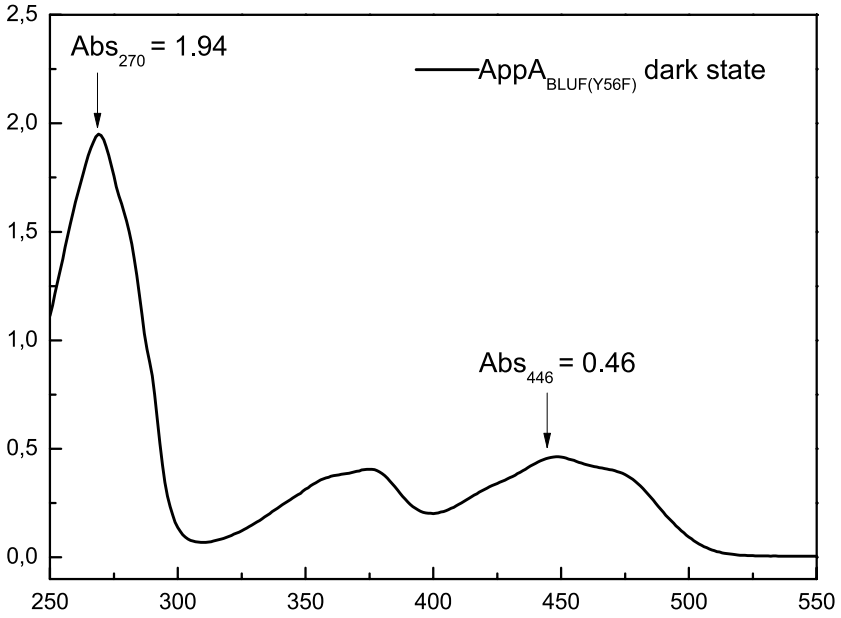

Figure S4. MALDI mass spectra showing 2-FY incorporation in AppA$_{BLUF(Y56F)}$.
The sample was digested with trypsin and treated with iodoacetamide to alkylate the cysteine residues. The calculated mass $[M+H]^+$ of the peptide containing 2-FY (GSHMLEADVTMTGSDLVSCC**Y**R) is 2507. The calculated mass of the native peptide containing the natural tyrosine is 2489. The area under the peak was used to calculate the percentage of a non-labeled protein in the sample, and indicated >96% incorporation of 2-FY into AppA$_{BLUF(Y56F)}$.

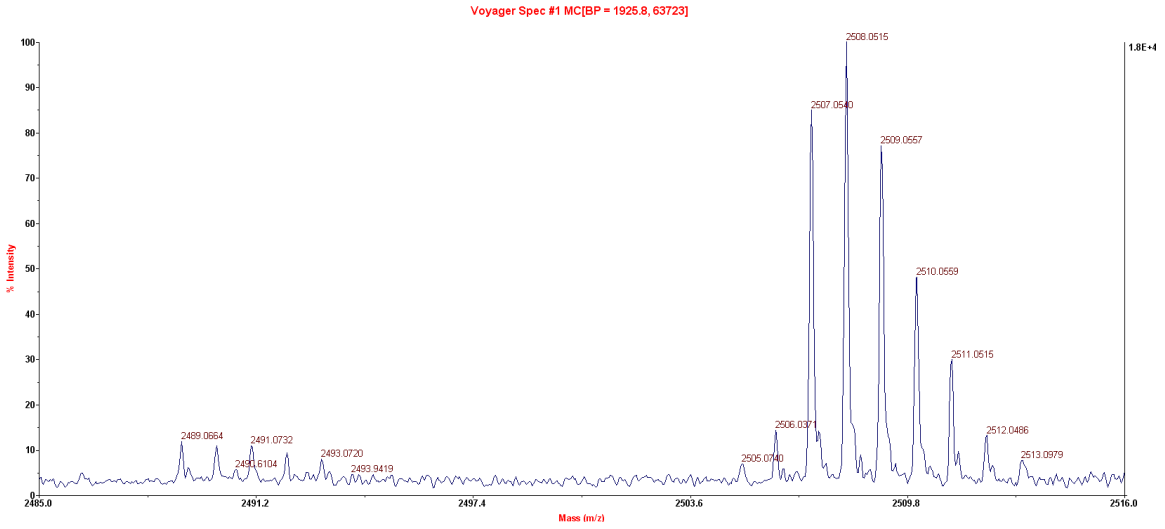

Figure S5. MALDI mass spectra showing incorporation of the 3FY, 2,3-F_2Y, 3,5-F_2Y and 2,3,5-F_3Y fluorotyrosines into App$A_{BLUF(Y56F)}$.

All samples were digested with trypsin and treated with iodoacetamide to alkylate the cysteine residues. The native peptide MQHDLEADVTMTGSDLVSCCYR has a calculated mass $[M+H]^+$ of 2588. However, the native peptide could only be detected in App$A_{BLUF(Y56F)}$ 3-FY21 at ~1% the intensity of the peptide arising from the labeled sample. Thus in all samples the incorporation of the fluorotyrosine is ≥99%.

A) App$A_{BLUF(Y56F)}$ 3-FY21:

The calculated mass $[M+H]^+$ of the 3-FY peptide is 2606.

B) AppA$_{BLUF(Y56F)}$ 2,3-F_2Y21

The calculated mass $[M+H]^+$ of the 2,3-F_2Y peptide is 2624.

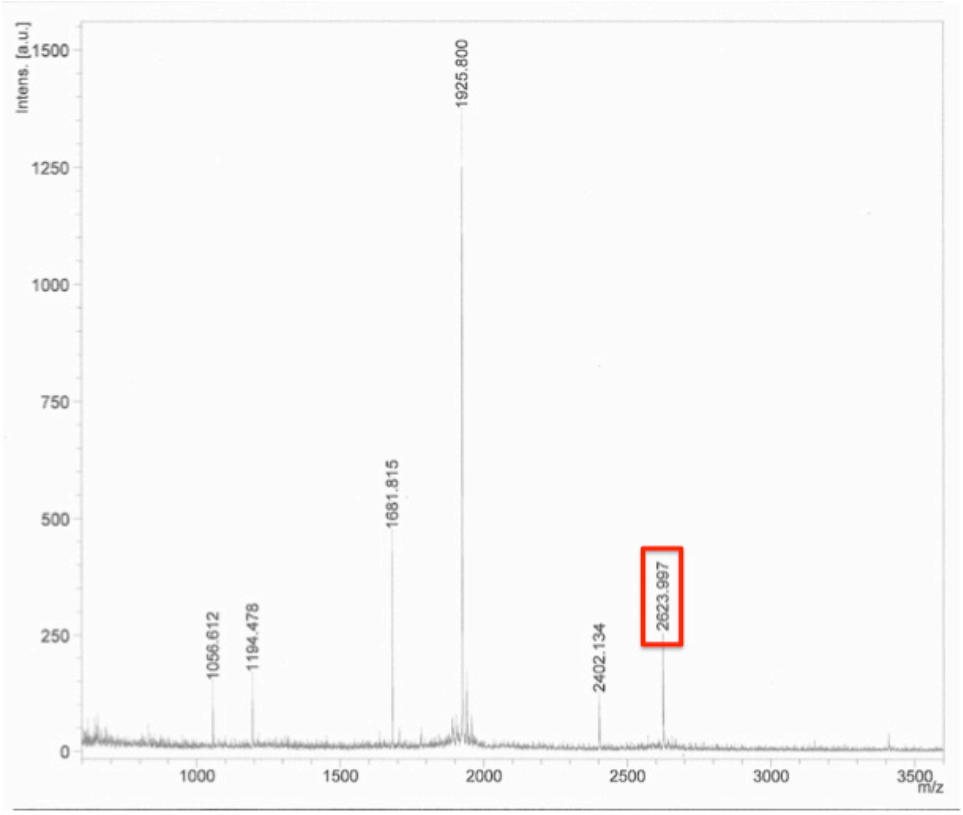

C) AppA$_{BLUF(Y56F)}$ 3,5-F_2Y21

The calculated mass $[M+H]^+$ of the 3,5-F_2Y peptide is 2624.

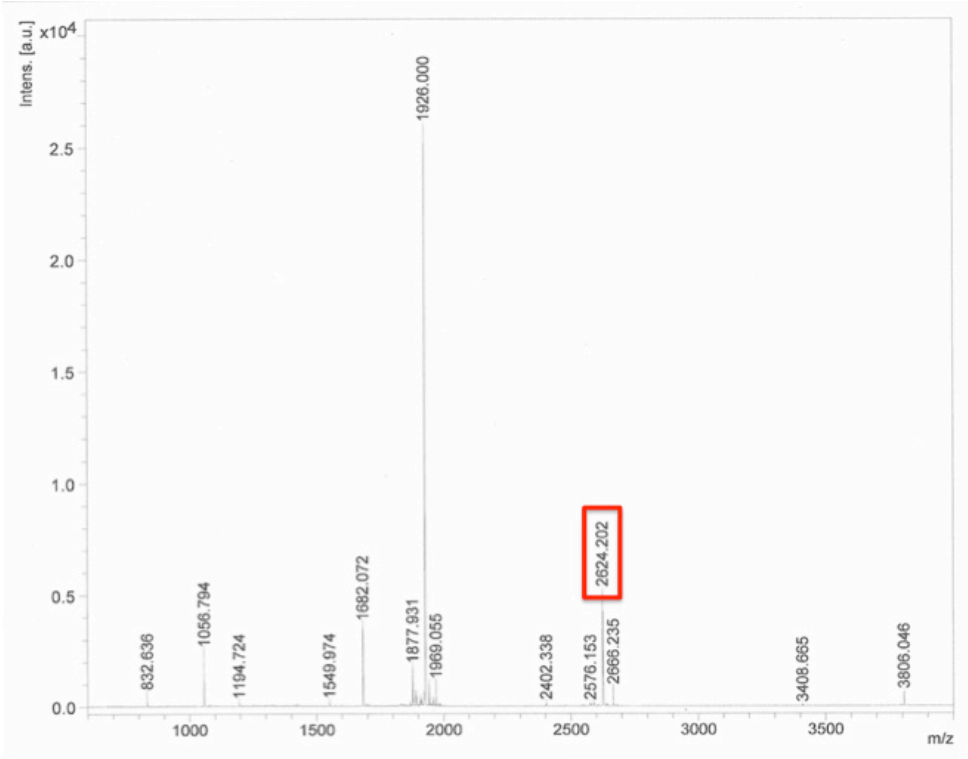

D) AppA$_{BLUF(Y56F)}$ 2,3,5-F$_3$Y21

The calculated mass $[M+H]^+$ of the 2,3,5-F$_3$Y peptide is 2642.

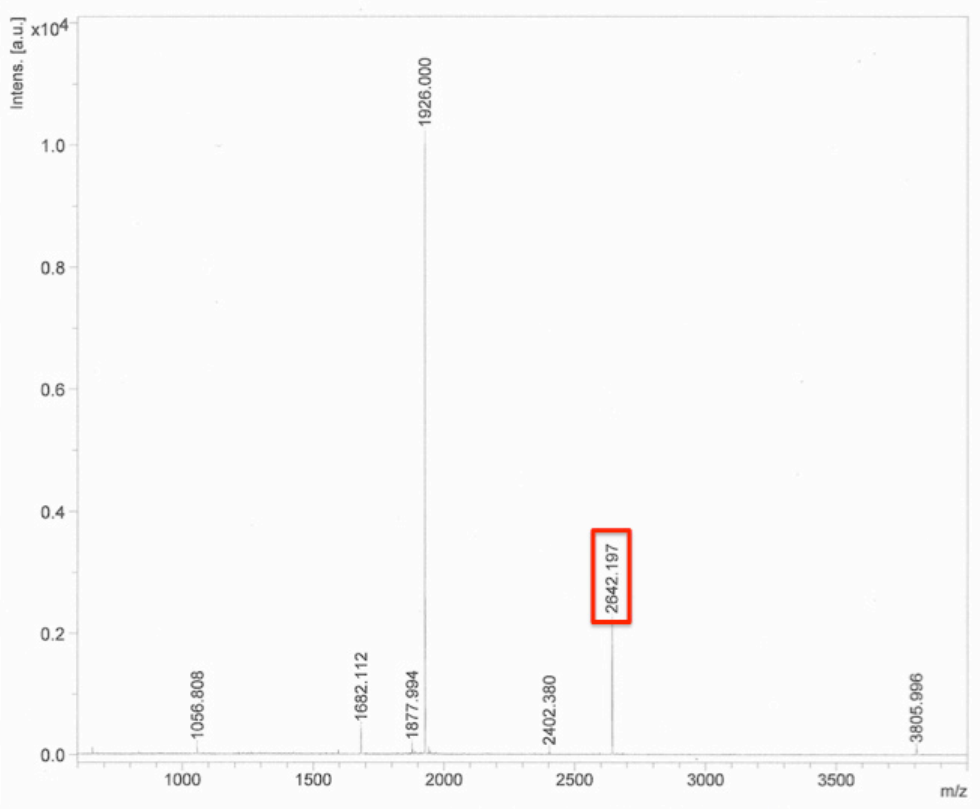

Figure S6. UV-Vis spectra recorded using the Ocean Optics USB2000+ spectrometer. A: Spectra of AppA_{BLUF} taken over a 2 hr period during continuous illumination with the white light source used to record the data. B: Absorbance at 450 nm recorded during continuous illumination with the white light source. A small increase in the amplitude is observed at 450 nm over the time course of irradiation. This is related to an increase in the background. Importantly these data show that the white light source does not result in formation of the light state or of the sample.

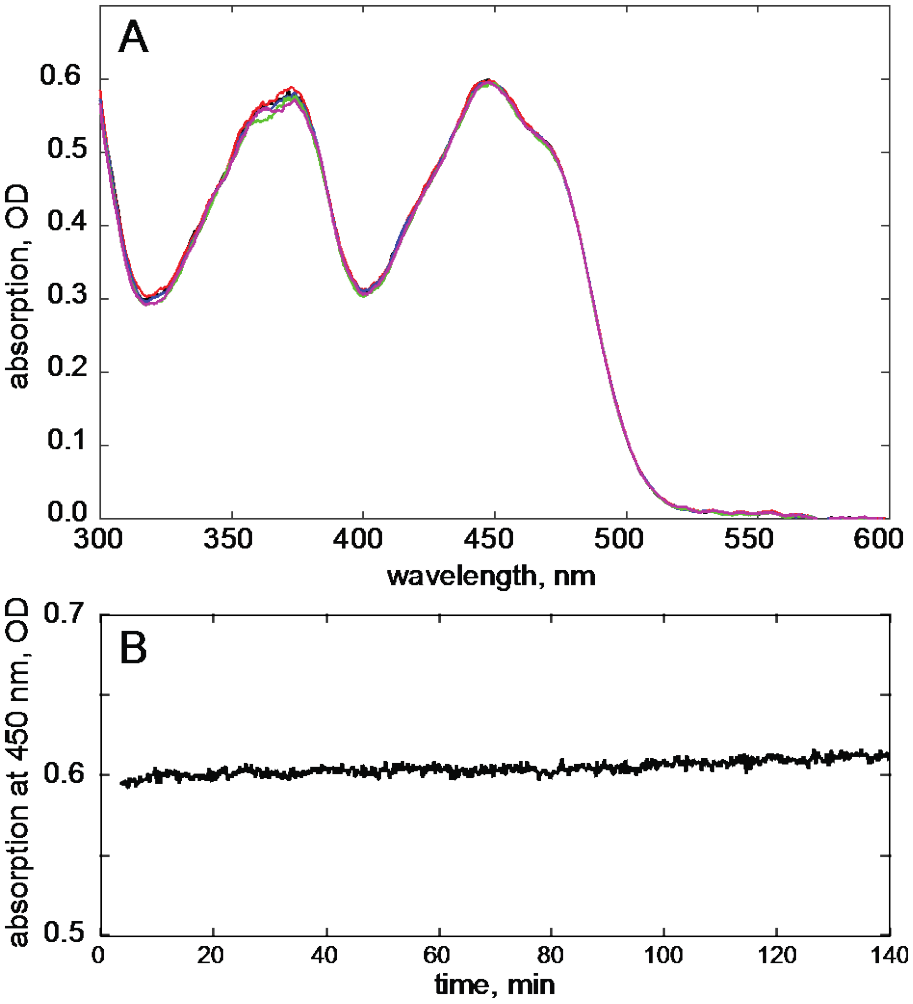

Figure S7. Comparison of the photoactivation portion of the photocycle of AppA$_{BLUF}$ and AppA$_{BLUF(Y56F)}$. In the EADS plot solid lines show wild-type AppA$_{BLUF}$ and dashed lines show AppA$_{BLUF(Y56F)}$. The spectral features and kinetic parameters confirmed that the Y56F mutation did not introduce changes to the structure nor the photoactivation of AppA$_{BLUF}$.

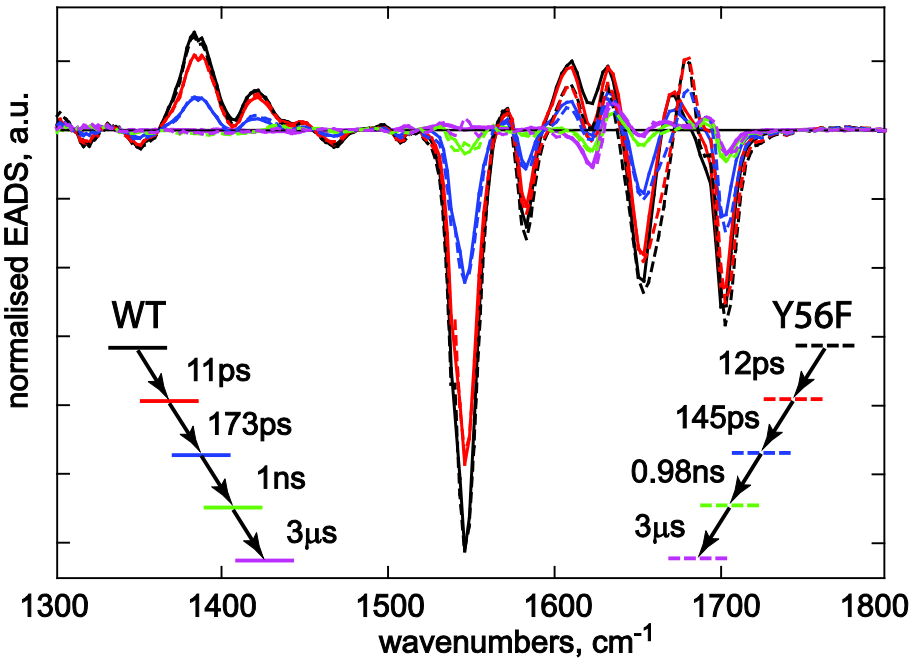

Figure S8. TRMPS dataset of AppA$_{BLUF}$ between 50 µs and 200 µs. These spectra support the observation that no further spectral evolution is observed on that time scale.

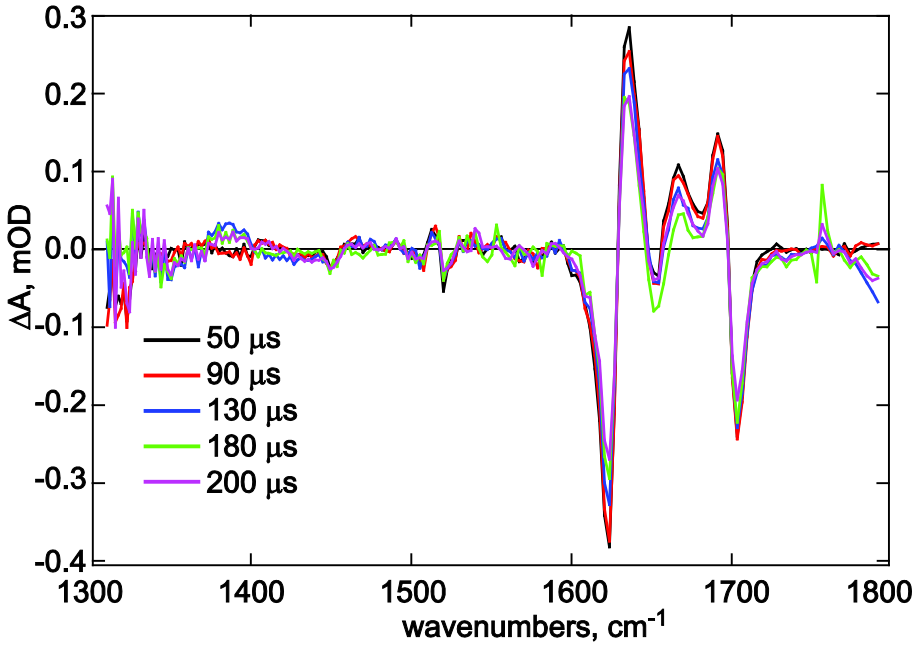

Figure S9. Complete TRMPS dataset of AppA$_{BLUF}$, AppA$_{BLUF(Y56F)}$, and the FY21 substituted AppA$_{BLUF(Y56F)}$. Left column shows the EADS spectra of all samples with estimated time constants and the right column shows the evolution of the experimental IR spectra as the protein is forming the light signaling state.

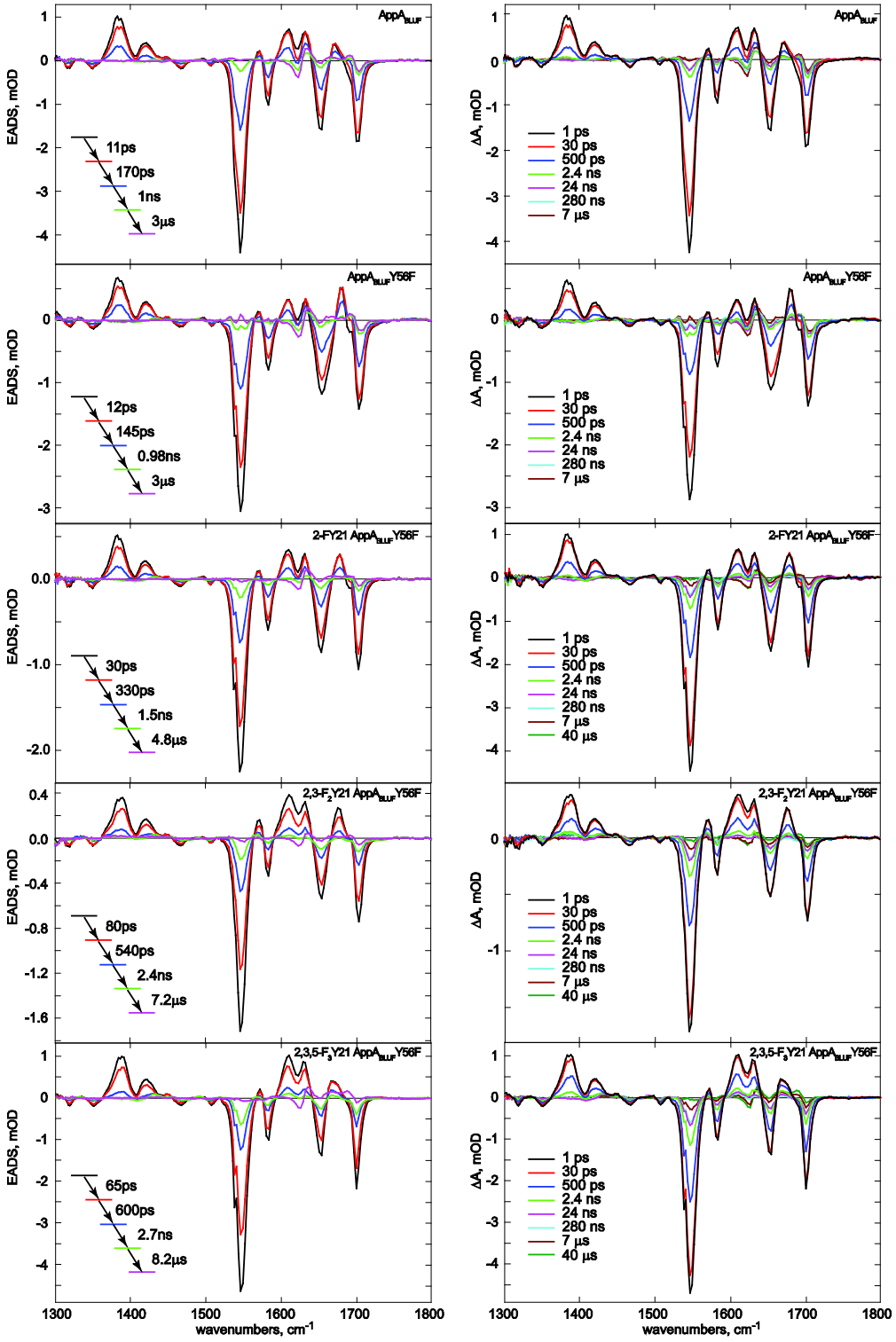

Figure S10. Rapid-scan FTIR difference spectra of AppA$_{BLUF(Y56F)}$ 2,3-F$_2$Y21. The recovery of the dark state was determined by analysis of the light minus dark state spectra. The estimated rate constant was determined from global analysis of the 1590 – 1710 cm^{-1} spectral region.